

^{31}P and ^1H NMR Studies of the Molecular Organization of Lipids in the Parallel Artificial Membrane Permeability Assay

Frauke Assmus,^{*,†,‡,§} Alfred Ross,^{||} Holger Fischer,[†] Joachim Seelig,[‡] and Anna Seelig[‡]

[†]Roche Pharmaceutical Research and Early Development, Pharmaceutical Sciences, Innovation Center Basel, F. Hoffmann-La Roche Ltd., Grenzacherstrasse 124, 4070 Basel, Switzerland

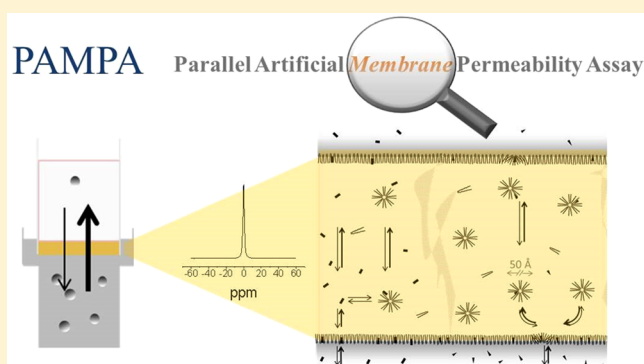
^{||}Roche Pharmaceutical Research and Early Development, Therapeutic Modalities, pCMC, Innovation Center Basel, F. Hoffmann-La Roche Ltd., Grenzacherstrasse 124, 4070 Basel, Switzerland

[‡]Division of Biophysical Chemistry, Biozentrum, University of Basel, Klingelbergstrasse 50/70, CH-4056 Basel, Switzerland

S Supporting Information

ABSTRACT: The parallel artificial membrane permeability assay (PAMPA) has emerged as a widely used primary *in vitro* screen for passive permeability of potential drug candidates. However, the molecular structure of the permeation barrier (consisting of a filter-supported dodecane–egg lecithin mixture) has never been characterized. Here, we investigated the long-range order of phospholipids in the PAMPA barrier by means of ^{31}P static solid-state NMR. Diffusion constants of PAMPA membrane components were derived from liquid state NMR and, in addition, drug distribution between the PAMPA lipid phase and buffer ($\log D_{\text{PAMPA}}$ at pH 7.4) was systematically investigated. Increasing concentration of *n*-dodecane to the system egg lecithin–water (lamellar phase, L_α) induces formation of inverted hexagonal (H_{ii}) and isotropic phases. At *n*-dodecane concentrations matching those used in PAMPA (9%, w/v) a purely “isotropic” phase was observed corresponding to lipid aggregates with a diameter in the range 4–7 nm. Drug distribution studies indicate that these reverse micelles facilitate the binding to, and in turn the permeation across, the PAMPA dodecane barrier, in particular for amphiphilic solutes. The proposed model for the molecular architecture and function of the PAMPA barrier provides a fundamental, hitherto missing framework to evaluate the scope but also limitations of PAMPA for the prediction of *in vivo* membrane permeability.

KEYWORDS: PAMPA, structure, NMR, membrane, phase transition



INTRODUCTION

Membrane permeability has been widely recognized as one of the core absorption, distribution, metabolism, excretion, and toxicity (ADME/TOX) parameters governing for example the extent of gastrointestinal drug absorption and permeation across the blood–brain barrier (BBB).¹ Early assessment of membrane permeability is therefore of great interest for the development and structural optimization of drug candidates.²

The extent of drug permeation depends on both the properties of the diffusing drug and the membrane. Biological membranes are highly ordered, anisotropic systems, made up of lipid bilayers into which proteins are embedded.³ The lipid composition determines the bilayer ordering and packing and thus—along with the activity of drug transporting proteins—the barrier properties of the membrane.

Various systems of different complexity have been used to mimic *in vivo* membrane properties and to experimentally determine a compound's permeability *in vitro*. Cell-based *in vitro* models (e.g., the CaCo-2 assay⁴) allow for the study of passive and active transport pathways in parallel, however, at

relatively low throughput and high implementation costs.⁵ As a higher throughput alternative, artificial membrane and membrane mimicking systems have gained high popularity for the screening of membrane binding and passive permeability. Similar to biological membranes, artificial membranes (e.g., liposomes, black lipid membranes (BLM)) are constituted of phospholipid bilayers to which a drug first binds by hydrophobic, hydrogen bonding, and ionic interactions, followed by permeation of the fraction of the drug that is uncharged at the particular pH. Measuring the partitioning into bulk organic phases (e.g., octanol) is a simpler approach, but fails to mimic the anisotropy of a bilayer as well as the charge of a phospholipid headgroup.

Structural differences between biological membranes and membrane surrogate systems have implications for the scope

Received: October 3, 2016

Revised: November 25, 2016

Accepted: December 1, 2016

Published: December 1, 2016



and limitation of the respective *in vitro* assay used for the prediction of relevant *in vivo* parameters. The linear relationship between octanol/water and phospholipid/water distribution coefficients, for example, breaks down for large, ionized and structurally diverse compounds.⁶ Interestingly, the molecular organization of the permeation barrier in the parallel artificial membrane permeability assay (PAMPA), one of the most commonly used systems for passive permeability screening, is still unresolved.

In PAMPA, a sandwich is formed consisting of an aqueous donor solution spiked with a test analyte, a permeation barrier, and an aqueous acceptor solution. The permeation barrier generally consists of synthetic or natural phospholipids dissolved in excess organic solvent and coated on a filter support (e.g., polyvinylidene difluoride (PVDF)).⁷ The assumption that bilayers may form in the PAMPA filter was based on previous work by Thompson et al., who investigated microfiltration units as stabilizing support for micro-BLM.⁸ By means of electrochemical measurements, the authors could show similarities between BLM and the microfilter–lipid system, suggesting that each pore in the filter was spanned by a single micro–lipid bilayer.⁸ The combination of solvent (*n*-decane), filter material (polytetrafluorethylene (PTFE), cellulose ester, polycarbonate), and lipid (egg phosphatidylcholine, cholesterol) studied by Thompson et al. has, however, never been applied for PAMPA. It is worth noting that recently a greater variety of filter materials has been investigated with respect to the ability to support membranes for biosensors.⁹ Evidence for the presence of micro-BLM in a PTFE but not a PVDF filter has been provided, yet the combination of phospholipid and solvent (*n*-octane) was again different from that used in PAMPA.

Notably, much effort has been put into optimization of the PAMPA setup, and specifically its barrier properties, in order to improve the prediction accuracy of, e.g., a drug's absorption potential and BBB permeation. To this purpose, individual components of the PAMPA barrier have been varied, including (i) the organic solvent (e.g., hexadecane,¹⁰ 1,7-octadiene¹¹), (ii) the lipid (1-palmitoyl-2-oleoylphosphatidylcholine (POPC), soy lecithin,¹² brain polar lipids, biomimetic lipid mixtures¹³), and (iii) the filter unit (PVDF,¹⁴ polycarbonate¹⁰). However, none of the optimization procedures included the inspection of the filter-supported barrier on a molecular level. Relationships found between lipid composition and bilayer membrane fluidity, on the one hand, and PAMPA permeability, on the other hand, relied on fluorescence anisotropy measurements of liposomes whereas anisotropy measurements of the PAMPA barrier itself failed.¹⁵ The influence of the presence of organic solvents and a filter support on the barrier properties was neglected. The molecular organization of lipids is likely to depend on the particular combination of filter, lipid, and organic solvent, and therefore none of the previous studies allowed conclusions on the molecular structure of the PAMPA barrier.

The purpose of this study was to investigate the lipid structure in the PAMPA barrier by means of solid-state ³¹P NMR and self-diffusion ¹H NMR experiments. Specifically we addressed the question whether the terms bilayer membrane and PAMPA membrane can be used synonymously. We centered our investigation around the PAMPA–lipid solution composed of a mixture of egg yolk lecithin (9%, w/v), cholesterol (0.45%, w/v), and excess *n*-dodecane, supported on a lipophilic PVDF filter.¹⁶ Solid-state ³¹P NMR measurements

were performed to study the long-range order of phospholipids and to allow a distinction between coarse dispersions of lipid bilayers, hexagonal phases, and lipid phases in which “isotropic” motion occurs.¹⁷ Moreover, the pulsed field gradient NMR (PFGNMR) technique (¹H NMR) was used to estimate individual diffusion coefficients in the PAMPA–lipid solution.¹⁸ In addition, the binding to and the permeability across the PAMPA barrier were measured for drugs of different charge state, lipophilicity, size, and concentration, and as a function of the egg lecithin content of the PAMPA barrier. Results are discussed in terms of the barrier properties and function of the PAMPA–lipid solution.

MATERIALS AND METHODS

Materials. Egg yolk lecithin (60% TLC), *n*-dodecane, deuterated *n*-dodecane-*d*₂₆, and diazepam were purchased from Sigma (Steinheim, Germany). POPC and phosphatidylethanolamine (PE) were obtained from Avanti Polar Lipids (Alabaster, Alabama). Propanolol was available through the Roche in-house Compound Depository Group as a proprietary compound. Tris and sodium chloride were obtained from Fluka (Buchs, Germany), and DMSO was purchased from Acros (Geel, Belgium). Formic acid, water, and acetonitrile were supplied from Merck (Darmstadt, Germany) and were of HPLC-grade.

³¹P NMR and ¹H NMR Studies. Sample Preparation. Samples for ³¹P NMR studies were prepared as follows: Lipid as a powder (egg yolk lecithin, pure POPC, or an egg yolk lecithin–cholesterol mixture) was dissolved in dichloromethane (52%, w/v), and the solvent was removed by rotary evaporation and subsequent high vacuum evaporation for >6 h. The dry lipid film was dispersed in buffer (50 mM Tris/114 mM NaCl, pH 7.4) at a molar phosphatidylcholine:water ratio of 1:45 (51 wt % water). The 50 mM Tris/114 mM NaCl buffer was prepared by adjusting with HCl to pH 7.4. Regarding the egg lecithin samples, the molar ratios referred to the amount of phosphatidylcholine present in the egg lecithin batch used (~60 wt %, for calculations of molar ratios, a molecular weight equal to that of POPC was assumed). The cholesterol content investigated was selected to match the concentration used in PAMPA (6 mol of phosphatidylcholine:1 mol of cholesterol).¹⁹ The lipid dispersion was covered with an argon, vortexed vigorously, and freeze–thawed in at least five cycles until no more sediments were visible by eye. Each freeze–thaw cycle consisted of three steps: freezing the sample in dry ice, warming it up to room temperature, and vortexing. Dodecane was added to the homogeneous lipid suspension up to the phosphatidylcholine:dodecane ratio typically used in PAMPA¹⁹ (0.25; 0.5; 1; 2; 3; 4; 5; 33.5 mol of dodecane per mol of phosphatidylcholine). The samples were vortexed, freeze–thawed, and vortexed again, and appropriate amounts were instantly transferred into 5 mm diameter glass tubes, which were flame-sealed. The samples were thermally equilibrated for at least 1 h before the measurements.

A second series of samples were prepared containing only egg lecithin and dodecane at the same phosphatidylcholine:dodecane ratios as described above. Dodecane was added directly to egg lecithin (no pretreatment with dichloromethane), and samples were vortexed, freeze–thawed, and transferred into the NMR tubes.

A third series of experiments were conducted with the egg lecithin–dodecane–cholesterol system prepared according to the protocol used for high throughput permeability measure-

ments¹⁹ and in the following referred to as “PAMPA–lipid solution”. To this purpose, a mixture of egg yolk lecithin (2.5 g), cholesterol (125 mg), and dodecane (25 mL) was stirred for >1 h, filtered (paper filter), and (i) transferred into an NMR tube without further treatment. In another setup, (ii) 40 PVDF filters (diameter 3 mm, punched out from a Millipore filter plate, MAIPN 4550) were subsequently coated with the PAMPA–lipid solution (4.5 μ L per filter) and stacked into an NMR tube. Moreover, (iii) PVDF filters were coated and stacked as described in (ii), but each PVDF layer was separated by a hydrophilic filter disk (punched out from a Millipore filter plate, MSGVN 22; impregnated with 5 μ L of H₂O).

It is worth to note that in the literature¹⁹ it has been specified that the PAMPA–lipid solution consists of 10% w/v egg lecithin and 0.5% w/v cholesterol dissolved in dodecane. However, adding egg lecithin to dodecane increases the volume of the resultant solution, which has not been considered so far for the calculations of egg lecithin and cholesterol concentrations. Following the above-mentioned protocol for the preparation of the PAMPA–lipid solution, and taking the volume change into account, results in the correct specifications which are 9% w/v egg lecithin and 0.45% w/v cholesterol in dodecane.

In analogy to the preparation of the PAMPA–lipid solution, samples for the diffusion experiments (¹H NMR) were prepared by adding 5 mL of perdeuterated dodecane to 0.5 g of egg yolk lecithin and 25 mg of cholesterol in a 10 mL glass flask. The mixture was vortexed thoroughly and filtered, and finally 600 μ L aliquots were filled in disposable 5 mm NMR tubes.

³¹P NMR. Static solid-state ³¹P NMR measurements were conducted at 298 K on a Bruker Avance 400 spectrometer (Bruker AXS, Karlsruhe, Germany) operating at a phosphorus-31 frequency of 162 MHz and using a pulse-acquire sequence with broadband proton decoupling (400 MHz). The recycling delay and the excitation pulse length were 6 s and 3 μ s, respectively. A typical spectrum was obtained from 500–12000 scans, depending on the lipid content of the sample.

¹H NMR Self-Diffusion Measurements. Translational diffusion coefficients of phosphatidylcholine, phosphatidylethanolamine, and cholesterol in the egg lecithin–cholesterol–dodecane-*d*₂₆ system (PAMPA–lipid solution) were determined using the pulsed field gradient technique (PFGNMR²⁰). Measurements were carried out on a Bruker 600-MHz Avance II spectrometer equipped with a cryogenic TCI probe head and a Bruker pulsed magnetic field gradient unit. Experiments were performed at 303 K with an internal lock on dodecane-*d*₂₆. Spectrometer operation and data processing were performed using Topspin 2.1 (Bruker, Fällanden, Switzerland). A pulsed gradient stimulated echo pulse sequence incorporating bipolar gradient pulses²¹ was used to generate the magnetic field gradient, which was ramped in 16 equidistant steps in a pseudo-2D experiment. The proton signals (i.e., the spin echo amplitudes) of phosphatidylcholine (chemical shift, δ = 3.42 ppm), phosphatidylethanolamine (δ = 1.62 ppm), cholesterol (δ = 0.77 ppm), and dodecane (δ = 0.87 ppm) were analyzed after Fourier transformation in the frequency domain.

In the presence of a gradient, molecular diffusion attenuates the ¹H signal amplitude, *I*, according to

$$I = I_0 \exp[-D\gamma^2 g^2 \delta^2 (\Delta - \delta/3 - \tau/2)] \quad (1)$$

where *I*₀ is the ¹H signal intensity in the absence of a gradient, *D* is the diffusion coefficient of the nuclei, γ is the gyromagnetic

ratio, *g* is the gradient strength (0–45 G cm^{−1}), δ is the duration of the pulse (δ = 1 ms), Δ is the interval between the gradient pulses (Δ = 300 ms), and τ is the time spacing between the individual bipolar gradient pulses (τ = 1 ms). Other parameters were as follows: 32k data points, 18 ppm spectroscopical line width, 1.5 s interscan delay, no H₂O suppression, exponential filtering (LB = 1 Hz), smoothed square gradient shape (SMSQ10.100), and manual baseline correction of the ¹H integral regions. Linear regression between the signal attenuation, $\ln I/I_0$, versus g^2 was performed to determine the slopes (slope_{lipid}, slope_{dodecane}) and corresponding diffusion coefficients (*D*_{lipid}, *D*_{dodecane}) of the individual lipid components. The diffusion constant of dodecane at 303 K (*D*_{dodecane} = 9.15 × 10^{−10} m² s^{−1}) was used to calibrate the magnitude of the field gradient pulses such that

$$D_{\text{lipid}} = \text{slope}_{\text{lipid}} \cdot D_{\text{dodecane}} / \text{slope}_{\text{dodecane}} \quad (2)$$

The *D* estimate for dodecane at 303 K was obtained by performing a linear regression on the known temperature-dependent self-diffusion constants of dodecane.²² Based on the assumption that the diffusing aggregates were spherical, apparent hydrodynamic radii (*r*₀) were obtained using the Stokes–Einstein equation:

$$D = \frac{kT}{6\pi\eta r_0} \quad (3)$$

where *k* is the Boltzmann constant (1.38 × 10^{−23} J K^{−1}), *T* is the temperature (303 K), and η is the solvent viscosity at 303 K (η = 1.24 mPa s, estimated from a biexponential fit of the known temperature dependent viscosities for dodecane²³).

Study of the Function of the PAMPA Barrier.
Measurement of PAMPA–Lipid Solution/Water Distribution Coefficients as a Function of Egg Lecithin Concentrations. Stock solutions of propranolol and diazepam in DMSO (10 mM and 2.5 mM) were diluted 1:100 with buffer (50 mM Tris/114 mM NaCl/pH 7.4) to obtain aqueous sample solutions (100 μ M and 25 μ M test compound, DMSO content 1%, v/v). The aqueous sample solutions (*V*_{aq} = 200 μ L) were transferred into an in-house made 96-well Teflon plate which was covered with a 96-well filter plate (PVDF, pore size 0.45 μ m, Millipore, Billerica, MA) precoated with PAMPA–lipid solution (*V*_{lipid} = 2.25 μ L). To investigate the influence of the egg lecithin concentration, PAMPA–lipid solutions containing 0–50 wt % egg yolk lecithin (Sigma) dissolved in dodecane were used (0; 1; 2; 3; 4; 5; 6; 7; 8; 9; 10; 12.5; 15; 17.5; 20; 22.5; 25; 30; 35; 40; 45; 50 wt %). It is important to note that the assay construct was designed such that the PAMPA–lipid solution was not in contact with the border of the Teflon well. The assembly was sealed and left undisturbed (room temperature) for at least 8 h, during which the solute was allowed to distribute. Time dependent measurements confirmed that equilibrium was reached within the 8 h incubation time (data not shown). After removal of the filter plate, equilibrium drug concentrations in the aqueous phase, *C*_{aq}^{eq}, were determined by means of HPLC–UV. PAMPA–lipid solution/water distribution coefficients were calculated by mass balance according to

$$\log D_{\text{PAMPA}} = \log \left(\frac{(C_{\text{aq}}^0 - C_{\text{aq}}^{\text{eq}}) V_{\text{aq}}}{C_{\text{aq}}^{\text{eq}} V_{\text{lipid}}} \right) \quad (4)$$

where *C*_{aq}⁰ is the initial aqueous drug concentration, which was obtained from a reference experiment carried out under the

same conditions but without coating the filter. A direct concentration analysis in both phases was not possible due to the inaccessibility of the PAMPA–lipid solution which resided in the pores of the PVDF filter. The term $\log D_{\text{PAMPA}}$ is therefore a composite parameter reflecting the drug distribution into PAMPA–lipid solution and drug adsorption to the filter-supported interface.

Measurement of PAMPA–Lipid Solution/Water Distribution Coefficients and Permeability for an Extended Data Set. Stock solutions of test compounds (10 mM) in DMSO were diluted with buffer (50 mM Tris/114 mM NaCl/pH 7.4) to obtain aqueous drug solutions (150 μM), which were filtered. The filtrate ($V_D = 320 \mu\text{L}$) was transferred into a Teflon donor plate and covered with a 96-well filter plate (PVDF, pore size 0.45 μm , Millipore, Billerica, MA) precoated with the PAMPA–lipid solution ($V_{\text{lipid}} = 4.5 \mu\text{L}$). In contrast to the measurements described in the previous section, blank assay buffer ($V_A = 280 \mu\text{L}$, 50 mM Tris/114 mM NaCl/pH 7.4) was added on top of the filter plate. After 19.5 h incubation, the sandwich was separated and the amount of drug in the acceptor and the donor solution was determined by comparison of the UV spectra with those from the initial filtrate (96-well UV plate reader, Molecular Devices, model Spectra Max 190, Sunnyvale, CA, and pION PSR4 p software). All measurements were performed in triplicate with an automated liquid handling system. For the calculation of the effective permeability (P_e), membrane retention was taken into account such that²⁴

$$P_e = \frac{2.303V_D}{A(t - t_s)} \left(\frac{1}{1 + V_D/V_A} \right) \log_{10} \left[1 - \left(\frac{1 + V_A/V_D}{1 - R} \right) \left(\frac{C_{A,t}}{C_{D,t=0}} \right) \right] \quad (5)$$

where A is the area of the filter (corrected for the apparent filter porosity, as described by ref 25), t the time, and t_s the time at steady state, V_D and V_A are the acceptor and the donor volumes, respectively, and $C_{A,t}$ and $C_{D,t}$ are the measured acceptor and donor concentrations, respectively, at time t . The PAMPA barrier retention factor R was obtained by mass balance according to

$$R = 1 - \left(\frac{C_{D,t} + (C_{A,t}V_A/V_D)}{C_{D,t=0}} \right) \quad (6)$$

$\log D_{\text{PAMPA}}$ was calculated as described in the previous section (eq 4), but here V_{aq} refers to the sum of V_D and V_A .

Measurement of Octanol/Water Distribution Coefficients and Ionization Constants. Octanol/water distribution coefficients, $\log D_{\text{oct}}$ (pH 7.4), were measured with a miniaturized filter-based shake flask assay (CAMDIS) as described elsewhere.²⁶ The same buffer as used for the measurement of $\log D_{\text{PAMPA}}$ values was applied (50 mM Tris/114 mM NaCl/pH 7.4). Ionization constants at $T = 25^\circ\text{C}$ and $I = 0.15 \text{ M}$ (aqueous solution) were measured by potentiometric titration as described elsewhere in more detail.²⁷

HPLC Instrumentation and Chromatographic Conditions. Drug concentrations in the aqueous phase were quantified using an Agilent 1290 Infinity HPLC-UV system. A 5 μL aliquot of each sample was injected onto a Kinetex 2.6 μm , 2.1 \times 50 mm analytical column. The flow rate was 2 mL/min, and the integrated column heater was set to 60 $^\circ\text{C}$. The mobile phase consisted of A (water) and B (acetonitrile), each

containing 0.1% (v/v) formic acid. The gradient elution was performed as follows: initial 2% B, 0–0.35 min linear gradient from 2% B to 95% B, 0.35–0.5 min 95% B, posttime 0.3 min. The gradient program for doxorubicin, vinblastine, buspirone, and colchicine was slightly different: initial 2% B, 0–0.5 min linear gradient from 2% B to 95% B, 0.5–0.65 min 95% B. Peak areas were recorded at an appropriate wavelength.

RESULTS

Characterization and Specification of Egg Lecithin.

The egg lecithin used in our studies, and commonly used for PAMPA permeability screening,¹⁹ was a yellow to orange colored, sticky material isolated from egg yolk and used as received from the supplier. In contrast to pure and well-defined lecithins like POPC, egg lecithin is a crude mixture of phospholipids, other lipids, and a variety of additional components such as triglycerides, sterols (e.g., cholesterol), fatty acids, glycolipids, and carbohydrates. The exact composition of egg lecithin depends on the stage of the purification process²⁸ and also varies batchwise. The composition of the egg lecithin used in our studies is given in Table 1 and relies on thin layer chromatography analysis provided by the supplier.

Table 1. Composition of Egg Lecithin “Powder” Used for Preparation of the PAMPA–Lipid Solution

component	fraction [wt %]
phospholipids	min 72
thereof	
phosphatidylcholine	min 59
phosphatidylethanolamine	min 6
lyso-phosphatidylcholine	max 3
other phospholipids	min 4
triglycerides	max 18
cholesterol	max 8
water	max 2

Characterization of the Filter. Like in most published PAMPA setups, a PVDF filter was used in this study as a support for the PAMPA–lipid solution. The filter was punched out from a Millipore filter plate commonly applied for the screening of passive permeability with PAMPA. The scanning electron micrograph (SEM) of the PVDF filter shown in Figure 1 demonstrates that the structure of the filter is highly porous, irregular in shape, and without any preferred orientation of the fibers. The pore size of the filter ranges from approximately 0.4 to 2.5 μm , showing that the nominal aperture (0.45 μm) is only a rough average.

NMR Studies of the Structure of the PAMPA Barrier.

Phase Equilibria in the System Egg Lecithin–Dodecane–Water (\pm Cholesterol). The first question we addressed in a series of ^{31}P NMR experiments was whether the commercial egg yolk lecithin is able to form lipid bilayers under optimal experimental conditions, i.e., in the presence of excess water (water:phosphatidylcholine ratio = 45:1 corresponding to 51 wt % water). Furthermore, we investigated the effect of increasing amounts of dodecane on the phase behavior of the egg lecithin– H_2O system up to the dodecane:phospholipid ratio typically used in PAMPA (33.5 mol of dodecane:1 mol of phosphatidylcholine, corresponding to 11.8 wt % egg lecithin). The effect of cholesterol (1 mol of cholesterol:6 mol of phosphatidylcholine) was investigated in parallel, taking into

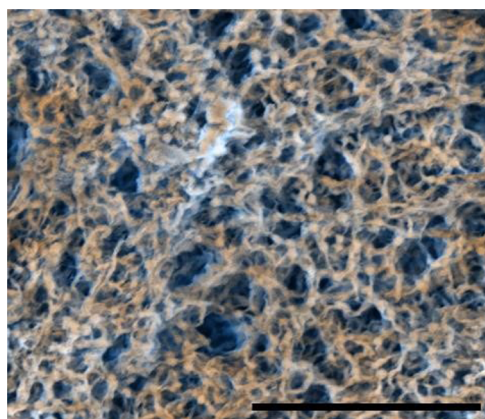


Figure 1. Scanning electron micrograph of the PVDF filter (Millipore, MAIPN) used in PAMPA. The length of the black line corresponds to 20 μm ; the nominal pore size was 0.45 μm .

consideration that the PAMPA barrier is commonly spiked with small quantities of cholesterol (0.45%, w/v).¹⁹

The ^{31}P NMR spectra of the egg lecithin– H_2O and the egg lecithin–cholesterol– H_2O system in the presence of increasing amounts of dodecane are shown in Figure 2. Generally, the spectra of both systems (with and without cholesterol) were almost superimposable, indicating that the applied quantities of cholesterol were too small to alter significantly the long-range order of the lipids.

In the absence of dodecane (Figure 2A) the line width, shape (low field shoulder and high field peak), and the residual chemical shielding anisotropy (approximately -50 ppm) of the spectra were characteristic for coarse dispersions of lipid bilayers. Upon addition of 0.25 mol (Figure 2B) and 0.5 mol (Figure 2C) of dodecane per mol of phosphatidylcholine, the

bilayer structure was essentially preserved, although a small isotropic line superimposed the bilayer spectra.

At 1 mol of dodecane per mol of phosphatidylcholine (Figure 2D), the ^{31}P NMR spectra corresponded to a pure hexagonal phase.¹⁷ Further addition of dodecane induced phase separation, which was macroscopically observed as islands of pure dodecane alongside the lipid dispersion. The ^{31}P NMR spectrum at a 2:1 dodecane/phosphatidylcholine molar ratio (Figure 2E) was a superimposition of all three types of spectra, namely, those of lipid bilayer, hexagonal phase, and isotropic phase. With increasing amounts of dodecane, the fraction of the “isotropic” phase increased at the expense of the lamellar and the hexagonal phase (Figure 2F–H). At a dodecane/phosphatidylcholine molar ratio of 33.5 (Figure 2I), which is the dodecane–lecithin ratio used in PAMPA,¹⁹ the ^{31}P chemical shielding anisotropy was averaged out and resulted in an isotropic peak.^{17,29}

In the above-described experiments, dodecane was subsequently added to the coarse bilayer dispersions. The ^{31}P NMR spectra of samples prepared in an inverse order (addition of water to the egg lecithin–dodecane mixture) were essentially identical (spectra not shown). When experiments were performed with pure POPC rather than egg yolk lecithin, the bilayer-type pattern of the POPC–buffer dispersion after the addition of dodecane was almost entirely preserved, except for the presence of a very small contribution of an isotropic phase at molar dodecane:POPC ratios $>0.5:1$ (see Supporting Information).

Phase Equilibria in the System Egg Lecithin–Dodecane. In the next series of experiments, dodecane was added directly to egg yolk lecithin without the addition of water, thus taking into account that also the bulk phase of the PAMPA barrier only contains moisture water. Moreover, no cholesterol was added since the homogeneity of an egg lecithin–cholesterol mixture

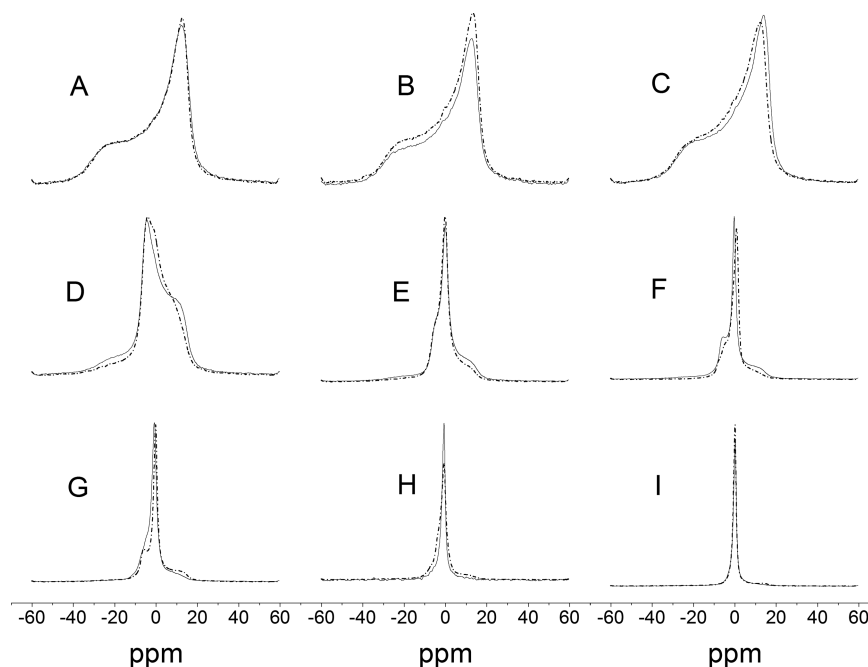


Figure 2. Pairwise superposition of experimental static solid state ^{31}P NMR spectra (recorded at 25 $^{\circ}\text{C}$) of egg lecithin containing 45 mol of H_2O per mol of lipid and increasing amounts of *n*-dodecane: 0 (A), 0.25 (B), 0.5 (C), 1 (D), 2 (E), 3 (F), 4 (G), 5 (H) and 33.5 (I) mol of dodecane/mol of phosphatidylcholine. Samples were prepared without (solid line) or with (dotted line) cholesterol (1 mol of cholesterol:6 mol of phosphatidylcholine).

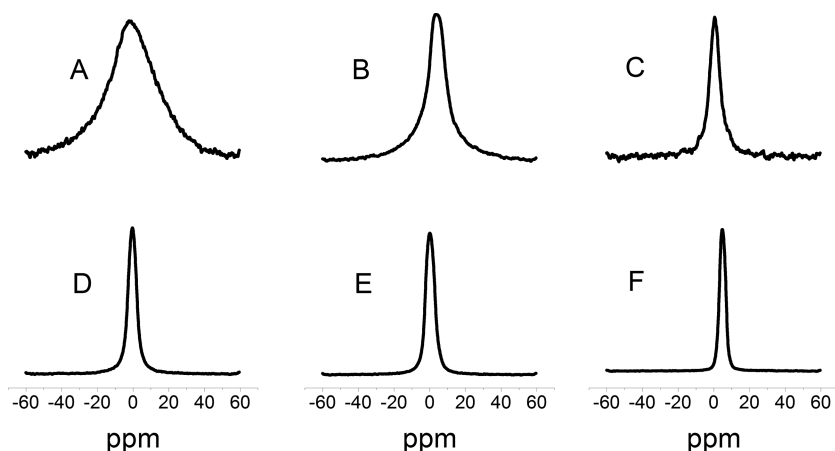


Figure 3. Experimental static solid state ^{31}P NMR spectra (recorded at 25 °C) of egg lecithin without additional H_2O and with increasing amounts of *n*-dodecane: 0 (A), 2 (B), 3 (C), 4 (D), 5 (E), and 33.5 (F) mol of dodecane/mol of phosphatidylcholine.

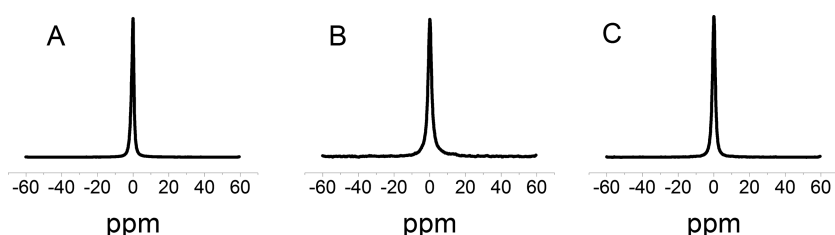


Figure 4. Experimental 162 MHz ^{31}P NMR spectra (recorded at 25 °C) of samples containing PAMPA-lipid (9% egg lecithin (w/v), 0.5% cholesterol (w/v)) in *n*-dodecane: (A) PAMPA-lipid solution without a filter device; (B) 40 stacks of hydrophobic PVDF filter devices (pore size 0.45 μm) impregnated with 4.5 μL of PAMPA-lipid solution per filter; (C) according to panel B, but each layer was separated by a hydrophilic PVDF filter device impregnated with 5 μL of H_2O .

without excess water would not be easily achieved at low dodecane concentrations. It is also important to note that the pretreatment of egg lecithin with dichloromethane following evaporation of the solvent (for facilitated mixing as described in the previous section) was not undertaken, in order to avoid altering the residual water content of egg lecithin.

An inspection of the ^{31}P NMR spectra of egg lecithin in the presence of dodecane shows that with increasing amounts of dodecane the line width narrows. The powder type of spectrum (Figure 3A) collapses into a classical isotropic peak characterizing the egg lecithin–dodecane mixture used in PAMPA (33.5 mol of dodecane per mol of phosphatidylcholine, Figure 3F).

Phase Equilibria in the System Egg Lecithin–Dodecane–Cholesterol (\pm Filter). The first two series of experiments have demonstrated that addition of a large excess of dodecane to egg lecithin (such as in PAMPA) induces the lamellar-to-isotropic phase transition, irrespective of the presence of excess water. However, lipid–organic solvent solutions containing as low as 2% (w/v) phospholipid are known to form bilayer membranes (BLM)³⁰ if painted across a smooth Teflon aperture immersed in water. In the next series of experiments we therefore tested whether the phase equilibrium of the PAMPA–lipid solution changes when coated across multiple apertures (i.e., the PVDF filter). Specifically we were interested if, in analogy to the formation of BLM, an isotropic-to-lamellar phase transition occurs.

Figure 4A and Figure 4B show the ^{31}P NMR spectra of the PAMPA–lipid solution either free in solution or coated on a PVDF filter. The spectra are essentially identical and correspond to an isotropic movement of the phospholipids. The separation of each phospholipid-coated PVDF filter with a

hydrophilic filter soaked with water (alternate stacking) did not change the pattern of the spectra (Figure 4C).

Diffusion Coefficient in the Isotropic Phase of the System Egg Lecithin–Dodecane–Cholesterol. The presence of an isotropic phase as observed in the ^{31}P NMR spectra of the PAMPA–lipid solution (Figure 5A–C) does not preclude the self-association of lipids and the formation of a definite microstructure.¹⁷ However, since the viscosity of the

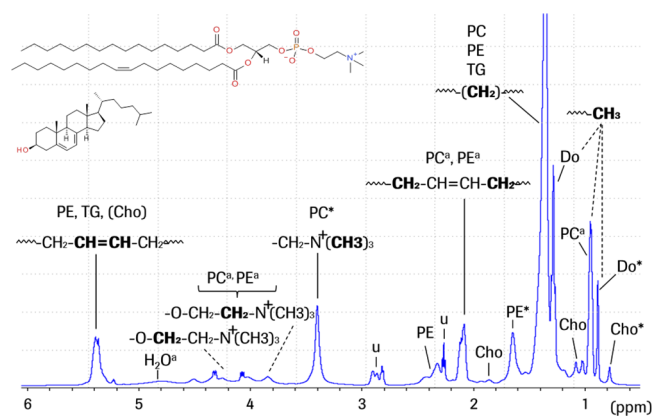


Figure 5. ^1H NMR spectra of the PAMPA–lipid solution (solvent: dodecane- d_{26}). PC: phosphatidylcholine. PE: phosphatidylethanolamine. Cho: cholesterol. TG: triglycerides. Do: dodecane. u: unidentified, additional components present. Structures of the main components (1-palmitoyl-2-oleoylphosphatidylcholine, cholesterol) in the PAMPA lipid solution are shown as insets.

Table 2. Diffusion Coefficients and Hydrodynamic Radii of Phosphatidylcholine (PC), Phosphatidylethanolamine (PE), and Cholesterol in the PAMPA Lipid Solution and 1:4, 1:16, and 1:64 Dilutions Thereof in Dodecane- d_{26}

dilution of the PAMPA–lipid soln	concn of egg lecithin in dodecane [%]	concn of cholesterol in dodecane [%]	app diff coeff ^a 10^{-12} [m ² s ⁻¹]			app hydrodynamic diam of the droplet [nm]		
			PC	PE	cholesterol	PC	PE	cholesterol
1:64	0.141	0.007	60.2	88.3	441.3	5.9	4.1	0.8
1:16	0.563	0.028	58.6	84.1	296.0	6.1	4.3	1.2
1:4	2.250	0.113	54.6	79.9	186.4	6.6	4.5	1.9
	9.000	0.450	52.1	78.1	102.5	6.9	4.6	3.5

^aThe diffusion coefficient of dodecane ($D_{\text{dodecane}} = 915 \times 10^{-12} \text{ m}^2 \text{ s}^{-1}$) was used as a calibrant.

PAMPA–lipid solution is low, it is safe to exclude that the observed isotropic peak corresponds to a cubic phase.

To further characterize the isotropic phase, translational diffusion coefficients of phosphatidylcholine (PC), phosphatidylethanolamine (PE), cholesterol, and dodecane in the egg lecithin–dodecane–cholesterol system were measured by means of ¹H NMR diffusion experiments. To this purpose, signals in the ¹H NMR spectrum of the PAMPA–lipid solution (egg lecithin–dodecane–cholesterol) were assigned to the individual lipid components. Due to the complex composition of egg lecithin, not all signals could be identified. Moreover, a number of peaks displayed a superposition of various components. For the diffusion experiments, spin echo decays were therefore analyzed for pure peaks or peak shoulders with a single diffusion pattern (Figure 5).

The influence of the egg lecithin concentration in dodecane on the individual diffusion coefficients was tested by performing experiments not only with the PAMPA–lipid solution but also with 1:4, 1:16, and 1:64 dilutions thereof in dodecane. Experimental spin echo decays of PC, PE, cholesterol, and dodecane- d_{26} as a function of the squared gradient strength (Stejskal–Tanner plot) are shown in the Supporting Information for the different egg lecithin concentrations. Diffusion constants were derived from the slopes and are listed in Table 2 along with the corresponding apparent hydrodynamic diameters of the diffusing objects. It is worth noting that the diffusion constant of dodecane was independent of the egg lecithin concentration, and therefore the average value for the diffusion constant of dodecane was used for calibration purposes (see Materials and Methods).

The rate of diffusion increased in the order PC < PE << cholesterol << dodecane, which corresponds to the reverse order of particle size. A clear trend toward decreasing rates of diffusion at increasing egg lecithin concentrations was evident, which was most pronounced for cholesterol. The diffusion coefficient of cholesterol in the undiluted and most diluted (1:64) PAMPA–lipid solution was, for example, 2-fold and 7-fold higher, respectively, as compared to that of PC. The sensitivity of the diffusion coefficient of cholesterol to the concentration of egg lecithin was reflected in the varying apparent hydrodynamic diameters ranging from 0.8 to 3.5 nm. The growth in aggregate size with an increase in the egg lecithin concentration was also observed for PE and PC, however, to a minor extent. Apparent hydrodynamic radii of PE aggregates (4.1–4.6 nm) were slightly lower than those of PC (5.9–6.9 nm), irrespective of the egg lecithin concentration used.

It is important to note that the echo decays of PE (see Supporting Information) deviated from a simple Gaussian diffusion behavior for which a straight line in the Stejskal–

Tanner plot would be expected. Nonspherical geometry of the diffusing particles and overlap of the selected PE signal with another component (either chemically different or another form of aggregate) could have contributed to the deviation. Moreover, it is noteworthy that measurements with a lipid-coated filter failed, due to severe line broadening which disturbed the homogeneity of the magnetic field.

Study of the Function of the PAMPA Barrier. *The Binding of Propranolol and Diazepam to the PAMPA–Lipid Solution.* While NMR studies gave insight into the molecular organization of lipids in the PAMPA permeation barrier, the functional role of lipids for the permeation process was investigated in the next step. To this purpose, the binding of drugs to the PAMPA–lipid phase was studied at two drug concentrations (100 μM and 25 μM) and as a function of the egg lecithin content in dodecane. Compounds of different charge state and lipophilicity were used as test compounds, i.e., diazepam as an example for a neutral lipophilic drug (basic $\text{pK}_a = 3.38$, $\log D_{\text{oct}}$ (pH 7.4) = 2.84) and propranolol as an example for a cationic compound with intermediate lipophilicity ($\text{pK}_a = 9.48$, $\log D_{\text{oct}}$ (pH 7.4) = 1.21). Mass balance derived distribution coefficients, $\log D_{\text{PAMPA}}$ (pH 7.4), for each drug concentration and as a function of the egg lecithin content are shown in Figure 6A and Figure 6B for propranolol and diazepam, respectively.

Generally, $\log D_{\text{PAMPA}}$ (pH 7.4) values increased with increasing concentrations of egg lecithin in dodecane. This “booster” effect of egg lecithin was notably more pronounced for propranolol as compared to diazepam. At egg lecithin concentrations >20%, $\log D_{\text{PAMPA}}$ (pH 7.4) values for propranolol were even higher than those for diazepam, despite comparably lower $\log D_{\text{oct}}$ and $\log D_{\text{PAMPA}}$ (pH 7.4) values assessed in pure organic solvents. The strongest effect of egg lecithin on $\log D_{\text{PAMPA}}$ (pH 7.4) values for propranolol was observed when increasing the egg lecithin concentration from 0 to 1%. This suggests that drug binding of propranolol to the PAMPA–lipid solution is mainly driven by the affinity to egg lecithin rather than dodecane.

It is also interesting to note that $\log D_{\text{PAMPA}}$ (pH 7.4) values for diazepam (neutral) were independent of the drug concentration applied, whereas lipid binding of propranolol (cationic) was the higher, the lower the drug concentration. Further investigation of the distribution behavior of propranolol over a wider concentration range ($C_{\text{aq}}^0 = 5\text{--}300 \mu\text{M}$) confirmed the trend toward lower $\log D_{\text{PAMPA}}$ (pH 7.4) values at higher drug concentrations (for details see Supporting Information).

Binding to and Permeation across the PAMPA Barrier for an Extended Data Set. Membrane binding is the first

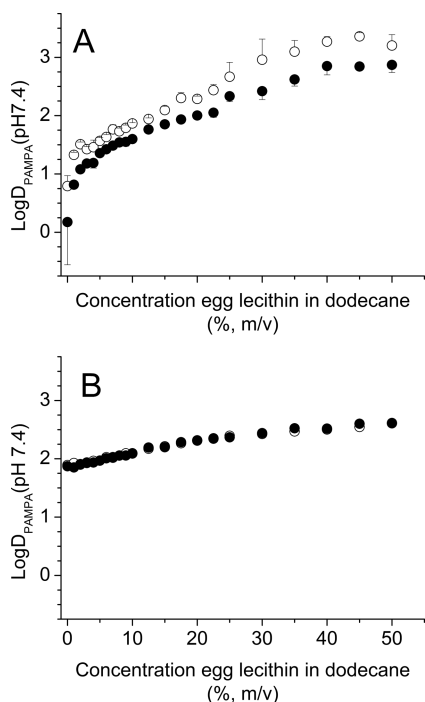


Figure 6. Egg lecithin–dodecane/buffer distribution coefficients, $\log D_{\text{PAMPA}}$ (pH 7.4), for (A) propranolol and (B) diazepam as a function of the amount of egg lecithin dissolved in dodecane. $\log D_{\text{PAMPA}}$ was measured at 25 μM (open circles) and 100 μM (closed circles) drug concentrations. Only one direction for the standard deviation is shown in A; the standard deviation in B is not shown as it was smaller than the size of the symbol.

step in the process of passive diffusion followed by permeation of the molecule across the membrane. In the next step, we therefore investigated the relationship between drug binding to and permeation across the PAMPA permeation barrier, with a particular focus on the role of molecular size and charge. To this purpose, $\log D_{\text{PAMPA}}$ (pH 7.4) and effective membrane permeability (P_e) values were measured for a structurally diverse 104-compound data set including acidic, basic, and noncharged drugs covering a large range of molecular size (cross sectional area, $A_D = 25\text{--}155 \text{ \AA}^2$, calculation of A_D according to ref 31) and lipophilicity ($\log D_{\text{oct}} = -1.15$ to

4.41). Physicochemical properties of all compounds along with measured $\log D_{\text{PAMPA}}$ (pH 7.4) values are provided in the Supporting Information. Moreover, $\log D_{\text{PAMPA}}$ (pH 7.4) and $\log D_{\text{oct}} - P_e$ values as a function of $\log D_{\text{oct}}$ (pH 7.4) are shown in Figure 7A and Figure 7B, respectively.

Despite the considerable scatter in the data, a linear relationship between $\log D_{\text{PAMPA}}$ (pH 7.4) and $\log D_{\text{oct}}$ (pH 7.4) was evident ($r^2 = 0.782$, standard deviation, $\text{SD} = 0.571$). Cationic drugs showed higher $\log D_{\text{PAMPA}}$ (pH 7.4) values than noncharged compounds with a similar $\log D_{\text{oct}}$ (pH 7.4), whereas anionic compounds were characterized by a lower membrane retention in the PAMPA permeation barrier. Interestingly, cationic compounds with low to intermediate lipophilicity ($\log D_{\text{oct}}$ (pH 7.4) < 1.5) were above the linear regression line and the line of identity, indicating their higher affinity to the PAMPA–lipid solution as compared to octanol ($\log D_{\text{PAMPA}} > \log D_{\text{oct}}$). In contrast, noncharged and anionic drugs as well as lipophilic cationic compounds showed higher $\log D_{\text{oct}}$ (pH 7.4) than $\log D_{\text{PAMPA}}$ (pH 7.4) values, with the exception of ketorolac, indomethacin, and theobromin (the exceptions are however close to the 1:1 line).

In order to evaluate the role of molecular size for the extent of binding to the PAMPA lipid solution in comparison to the distribution into bulk octanol, $\log D_{\text{PAMPA}}$ and $\log D_{\text{oct}}$ values should be compared for noncharged compounds only. This circumvents the problem of concentration dependent effects and takes into account that initial drug concentrations differed according to drug solubility. An inspection of the $\log D_{\text{PAMPA}} - \log D_{\text{oct}}$ relationship for noncharged drugs reveals a linear trend indicating that large molecules are equally well accommodated in the PAMPA barrier and in the bulk phase of an organic solvent (octanol). The compound with the largest cross sectional area, for example (i.e., paclitaxel, $A_D = 155 \text{ \AA}^2$), did not deviate from the linear regression line, and only a slight discrepancy was observed for ritonavir ($A_D = 121 \text{ \AA}^2$) and indinavir ($A_D = 125 \text{ \AA}^2$).

The above-described linear relationship between $\log D_{\text{PAMPA}}$ (pH 7.4) and $\log D_{\text{oct}}$ (pH 7.4) is interestingly not reflected in the bilinear relationship between P_e and $\log D_{\text{oct}}$ (pH 7.4) shown in Figure 7B. It can therefore be excluded that the decrease of P_e with an increase in $\log D_{\text{oct}}$ (pH 7.4) at $\log D_{\text{oct}} > 3$ (i.e., when compounds become increasingly large) is due to a

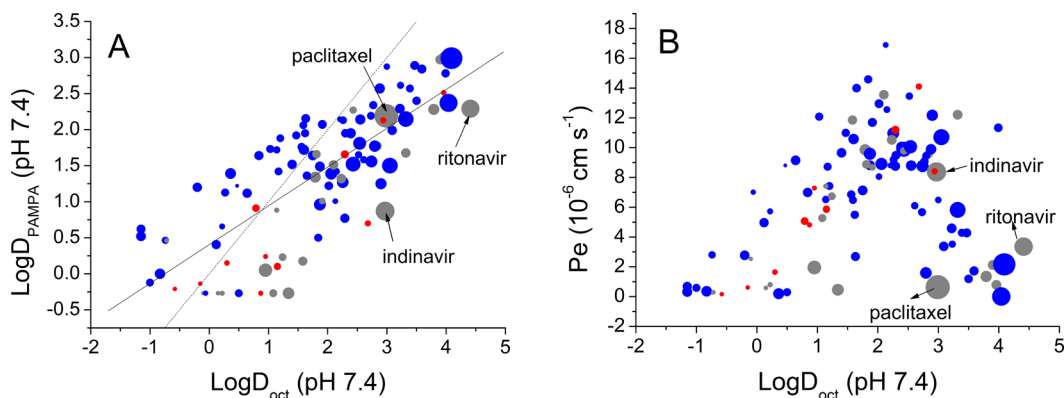


Figure 7. (A) Relationship between the PAMPA–lipid solution/water distribution coefficients, $\log D_{\text{PAMPA}}$ (pH 7.4), and octanol/water distribution coefficients, $\log D_{\text{oct}}$ (pH 7.4), for a set of 104 structurally diverse drugs. (Dotted line) line of identity, (solid line) linear regression line (correlation statistics: $\log D_{\text{PAMPA}} = 0.538 \log D_{\text{oct}} + 0.405$ ($n = 104$, $r^2 = 0.782$, $\text{SD} = 0.571$)). (B) Relationship between the effective permeability, P_e , across the PAMPA barrier and $\log D_{\text{oct}}$ for the same data set. Colors according to charge class: nonionic (gray circles), cationic (blue circles), anionic (red circles); size according to the cross sectional area, A_D , of the drug.

greater resistance of the PAMPA barrier to the binding of compounds with increasing molecular size.

■ DISCUSSION

In order to assess the scope and limitation of an *in vitro* permeability assay for the prediction of *in vivo* membrane permeability, an understanding of the structure and properties of the applied membrane mimicking system is fundamental. In this study, the structure of the PAMPA permeation barrier has been investigated by means of ^{31}P NMR and ^1H NMR, which gave insight into the organization of lipids at the molecular level. Moreover, the role of drug concentration, molecular size, and charge for the binding to and permeation across the PAMPA barrier have been investigated. The results will be discussed in terms of the structure and function of the egg lecithin–dodecane–filter system used in PAMPA, and a model for permeation mechanisms across the PAMPA barrier will be proposed.

The Structure of the PAMPA Barrier. The Instability of a Bilayer in the Presence of Excess Dodecane. One major difference between the composition of biological membranes and the PAMPA barrier is the presence of excess dodecane in PAMPA.¹⁴ Previous studies investigated the effect of dodecane up to 2 mol of dodecane:1 mol of pure phospholipid only. Here we expanded our investigation to the dodecane:phosphatidylcholine ratio used in PAMPA (i.e., 33.5 mol of dodecane:1 mol of phosphatidylcholine). Our results at low dodecane concentrations were in line with the literature^{32–34} and showed that dodecane promotes the inversion from a bilayer (L_α) to an inverted hexagonal (H_{II}) phase. However, higher dodecane concentrations (>10 mol %) induced the formation of an isotropic phase, irrespective of whether cholesterol, water, or a filter support for the lipid mixture were present. Previous studies, relying on liposomes as surrogate systems for the barrier fluidity and permeability in PAMPA, are therefore of limited value, and derived guidelines for the optimization of PAMPA may need to be considered carefully.¹⁵

The Influence of the Filter. The absence of bilayers in the PAMPA barrier may at first be surprising since Thompson et al.³⁵ provided evidence for the existence of micro-BLM in filter-supported lipid–solvent systems. Much of Thompson's line of argument relied on the observed increase of micro-BML conductivity upon addition of amphotericin, a peptide spanning exactly one leaflet of a bilayer membrane. However, the filter used in Thompson's experiments was polycarbonate, characterized by a highly uniform series of holes and separated by a smooth, nonporous polymer.³⁵ In contrast, the SEM image of the PVDF filter applied in PAMPA (Figure 1) demonstrates the rough surface of PVDF.

More recently, Phung et al.⁹ tested the ability of various filter materials to support BLMs for biosensors and could show that PVDF does not support bilayers (the authors used a different lipid–solvent mixture than in PAMPA: 5% (w/w) PC and 2% (w/w) cholesterol dissolved in *n*-octane). NMR studies of the PAMPA filter performed in this study confirmed that PVDF is unfavorable for providing an aperture for BLM. The lack of BLM formation may be attributed not only to the roughness of the PAMPA filter but also to the relative hydrophilicity of PVDF as compared to, e.g., Teflon (PTFE). Ever since the pioneering work of Montal and Müller, hydrophobic surfaces have been preferred for the formation of BLM.³⁶

The Influence of the Lipid Composition. Previous studies of the dodecane–lecithin system have focused on pure lipid

species (POPC; 1,2-dioleoyl-*sn*-glycero-3-phosphocholine [DOPC]^{32,33}) differing from crude extracts of egg yolk commonly used for PAMPA.¹⁹ Our results demonstrated that crude egg lecithin bilayers are more prone to undergo the lamellar-to-isotropic phase transition as compared to pure POPC, pointing to a higher instability of egg yolk lecithin bilayers (Figure 2 and Figure S1).

A Model for the Structure of the PAMPA Barrier. In order to further characterize the nature of the isotropic phase, self-diffusion coefficients for individual components of the PAMPA–lipid solution were measured. The diameters for PC and PE aggregates ($d = 6.9$ and 4.6 nm, respectively, in undiluted PAMPA–lipid solution) can be explained by the presence of reverse micelles. Due to the low water content, phospholipids in the PAMPA–lipid solution most likely orient themselves with the headgroup toward the residual water (maximal 2%, according to the supplier) and the tails pointing toward the surrounding dodecane phase.

The fast diffusion coefficient measured for dodecane suggests that the largest part of the solvent is not incorporated in micelles, but that bulk dodecane surrounds the lipid micelles. Likewise, cholesterol appears not to be completely incorporated in the reverse micellar structure, as indicated by the diffusion coefficient of cholesterol in the intermediate range between those for dodecane and PC/PE.

Notably, the determined diffusion coefficients are an average for the different physical states of a chemically defined species, weighted according to the relative proportion of that physical state. This means that the coexistence of monomers and lipid aggregates gives rise to an average diffusion coefficient and, in turn, an average estimate for the aggregate diameter. In the undiluted PAMPA–lipid solution, the proportion of the monomeric form of phospholipids is the lowest, and accordingly the influence on the diffusion coefficient is the smallest. Thus, the estimate for the diffusion coefficients in the undiluted PAMPA–lipid solution should yield a reasonable approximation for the diameter of the reverse micelles.

Yet, it is important to note that another simplification was made by using the Stokes–Einstein equation to estimate diameters of the diffusing lipid aggregates. This approach is based on the assumption of spherical particles, however the nonlinearity in the spin echo decays (see [Supporting Information](#)) could be explained by either the presence of nonspherical particles or a mixture of spherical particles with different sizes. Nevertheless, this applied model provides reasonable estimates for the lipid aggregate size.

The presence of reverse micelles is in line with a large body of knowledge about the organization of amphiphiles (e.g., phospholipids) in nonpolar organic solvents (best characterized solvent: cyclohexane).³⁷ In qualitative terms, such systems correspond to the PAMPA–lipid solution before its coating on a filter support. Purified phospholipids have been shown to assemble into spherical reverse micelles, which transform into reverse tubular structures (micrometer range) upon addition of low amounts of water. These wormlike micelles are assumed to entangle and form continuous three-dimensional networks with pronounced gel properties.^{38–41} Since the PAMPA–lipid solution is not gel-like, the formation of a network of wormlike micelles is unlikely. This is in line with literature reporting that purified but not crude soy lecithin dissolved in dodecane undergoes the liquid-to-gel transition.⁴² However, the presence of short wormlike micelles in the PAMPA–lipid solution

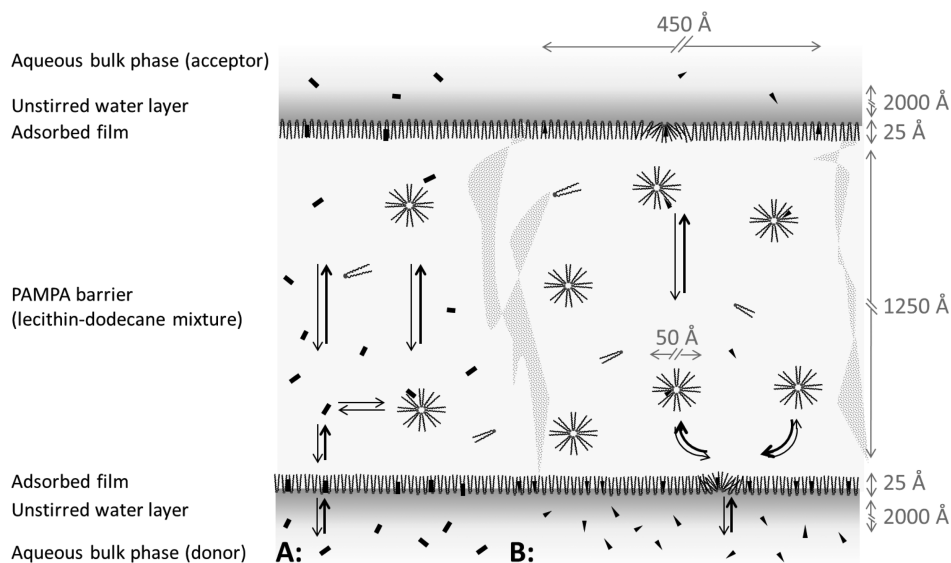


Figure 8. Hypothesized structure of the PAMPA barrier and two proposed mechanisms of transport. (A) Penetration across the PAMPA–lipid solution/water interface and transport via the continuous dodecane phase. In the dodecane phase, the solute may also bind to inverted micelles diffusing across the membrane to the acceptor site of the PAMPA–lipid solution/water interface. The mechanism is assumed to play an important role for compounds with high solubility in dodecane (black rods). (B) Formation of hemimicelle-like structures at the PAMPA–lipid solution/water interface consisting of phospholipids that accommodate the solute. Drug-loaded reverse micelles may detach from the interface at the donor site and diffuse across the membrane to the acceptor site. There, the solute may be released by the same mechanisms proceeding in reverse order. Mechanism B is assumed to play a crucial role for the transport of amphiphilic drugs with low solubility in dodecane (black triangles). Light gray regions with an irregular shape denote the PVDF filter support.

cannot be excluded and could be an explanation for the deviation from linearity in the spin echo decays.

The self-diffusion NMR experiments of the PAMPA–lipid solution were conducted without a filter support due to the disturbance of the magnetic field and the associated severe line broadening in high resolution NMR. We cannot rule out that the filter changes the size of the aggregates, however, the ^{31}P NMR in the presence of a filter clearly demonstrated that the lipid aggregates tumble rapidly with respect to the time scale of NMR. Moreover, the estimated size of the micelles (6.9 nm) is manifold smaller than the size of the pores in a PAMPA filter (0.45 μm), which suggests that the results are also applicable to the filter–phospholipid–solvent system.

The Function of Lipids in the PAMPA Barrier and a Proposed Permeation Mechanism. Distribution studies of propranolol and diazepam showed that the higher the egg lecithin content in the PAMPA barrier, the higher the distribution coefficient, which points to a carrier role of the phospholipids. For propranolol (cationic amphiphilic), the increase in the distribution coefficient was exceptionally high when increasing the egg lecithin content from 0 to 1%. This indicates a change in the binding mechanism in the presence of egg lecithin that most likely reflects the solubilization of amphiphilic drug in reverse micelles. For propranolol, a more pronounced increase in $\log D_{\text{PAMPA}}$ (pH 7.4) with increasing concentrations of egg lecithin was observed as compared to diazepam. This suggests that amphiphilic molecules with intermediate lipophilicity show a higher affinity to the inverted egg lecithin micelles whereas lipophilic, nonamphiphilic solutes (e.g., diazepam) are already well solubilized by dodecane.

Apart from drug distribution into the bulk phase of the PAMPA–lipid solution, the relevance of interfacial drug adsorption can be inferred from the observed trend toward lower $\log D_{\text{PAMPA}}$ (pH 7.4) values at higher drug concentrations. The same pattern observed for the binding of

propranolol to the PAMPA–lipid solution is well-known from drug binding studies to lipid bilayers.³⁵ The insertion of cationic drugs, such as propranolol, into electrically neutral lipid bilayers creates a positive surface potential, Ψ_0 , which leads to the repulsion of molecules with the same charge. Therefore, surface distribution becomes increasingly difficult at higher drug concentrations, resulting in decreasing apparent binding constants (or here decreasing $\log D_{\text{PAMPA}}$ = interfacial + bulk phase drug distribution). Electrostatic repulsion and saturation effects may notably occur not only at the PAMPA–lipid solution/water interface but also at interfaces present in the bulk phase of the lipid mixture.

Considering the amphiphilic nature of phospholipids, it can be assumed that not only the amphiphilic drug but also egg lecithin resides at the PAMPA–lipid solution/water interface. The formation of a monolayer or a monolayer in addition to multiple bilayers is plausible. However, due to the large excess of the bulk lipid phase (bulk lipid:interface $\sim 3000:1$), the presence of lipids aligned in a membrane leaflet could not be verified by means of ^{31}P NMR.

It is well established that the energy (ΔW) required to form a cavity in a lipid monolayer or a lipid membrane, large enough to accommodate the solute, is proportional to the lateral packing density of the lipid layer (π_{M}) and the cross sectional area (A_{D}) of the penetrating compound ($\Delta W = \pi_{\text{M}}A_{\text{D}}$).^{6,43} This explains the increasing resistance of densely packed (solvent-free) membranes with increasing lipid chain ordering and permeant size.^{1,44} Following a comparison with drug distribution into bulk octanol (see also ref 6), an attenuated insertion of large molecules in the PAMPA–lipid solution was not observed, again pointing to a less structured nature of the PAMPA–lipid solution/water interface as compared to densely packed biological membranes. It can therefore be excluded that the bilinear relationship between P_e and $\log D_{\text{oct}}$ (pH 7.4), typically found in unstirred PAMPA measurements (see also

Figure 7B), is due to a size restriction of the PAMPA permeation barrier. The main reason for the observed bilinearity is rather the presence of the unstirred water layer,⁴⁵ which limits the diffusion of lipophilic compounds.

The above-described considerations about the structure and the function of lipids in the PAMPA permeation barrier are summarized in Figure 8. The cartoon shows the proposed mechanism of transport for lipophilic compounds and amphiphilic compounds with intermediate lipophilicity across the PAMPA layer via inverted micelles.

Limitations, Future Perspectives, and Recommendations. We could show that the addition of excess dodecane to coarse dispersions of egg lecithin bilayers promotes a lamellar-to-isotropic phase transition, irrespective of the presence of water, cholesterol, or a filter support. Our study, however, only focused on the filter most commonly used in PAMPA, i.e., PVDF, whereas it remains to be investigated whether the results can be applied to other filter types. Moreover, the commonly used crude extract of egg lecithin was used to prepare the PAMPA–lipid solution. Further research may thus be required to investigate the phase behavior of, e.g., pure POPC–dodecane solutions in the presence of a filter. Moreover, self-diffusion NMR studies gave only approximate estimates for the diameter of the diffusing aggregates, and a more detailed analysis is needed to provide further insight into the shape of the lipid aggregates.

Our findings may be useful for re-evaluation and interpretation of PAMPA permeabilities measured in previous studies. The permeation of ionized species, for example, observed in PAMPA experiments^{46–49} cannot easily be applied to the permeation across the hydrophobic core of a phospholipid bilayer present in biological membranes. Moreover, permeability data from stirred PAMPA experiments need to be considered carefully for *in vitro* to *in vivo* extrapolation approaches since membrane permeation of bulky compounds is overestimated in PAMPA.

CONCLUSION

In summary, our NMR studies indicated that reverse micelles are formed in the bulk phase of the PAMPA permeation barrier whereas the existence of lipid bilayers could not be verified. The presence of egg lecithin facilitates drug binding to the PAMPA–lipid solution, suggesting that inverted micelles act as a carrier, rather than as a barrier, in the process of drug permeation. As distinct from densely packed biological membranes, attenuated insertion of large compounds into the PAMPA–lipid solution was not observed. The new insights into the structure and function of the PAMPA permeation barrier provide a useful framework to evaluate the scope but also limitations of PAMPA for the prediction of *in vivo* membrane permeability.

ASSOCIATED CONTENT

Supporting Information

The Supporting Information is available free of charge on the ACS Publications website at DOI: 10.1021/acs.molpharmaceut.6b00889.

³¹P NMR spectra, experimental spin echo decays, binding of propranolol to the PAMPA lipid solution, physicochemical properties, and PAMPA–lipid solution/water distribution coefficients (PDF)

AUTHOR INFORMATION

Corresponding Author

*Phone: +49 17622960169. E-mail: frauke_assmus@hotmail.com.

ORCID

Frauke Assmus: 0000-0002-1146-3452

Present Address

[§]F.A.: Department of Molecular Epidemiology, German Institute of Human Nutrition Potsdam-Rehbruecke, Arthur-Scheunert-Allee 114–116, 14558 Nuthetal, Germany.

Notes

The authors declare no competing financial interest.

ACKNOWLEDGMENTS

We thank André Ziegler and Christian Müller for help with running the ³¹P solid state NMR experiments and Marta Hidalgo for help with the preparation of the lipid samples. Moreover, we thank Matthias Lauer for performing the SEM imaging experiments and for fruitful discussions.

REFERENCES

- (1) Fischer, H.; Gottschlich, R.; Seelig, A. Blood-brain barrier permeation: molecular parameters governing passive diffusion. *J. Membr. Biol.* **1998**, *165* (3), 201–211.
- (2) Poole, S. K.; Poole, C. F. Separation methods for estimating octanol-water partition coefficients. *J. Chromatogr. B: Anal. Technol. Biomed. Life Sci.* **2003**, *797* (1–2), 3–19.
- (3) Seelig, A.; Seelig, J. Membrane Structure. *Encycl. Phys. Sci. Technol.* **2002**, *9*, 355–367.
- (4) Artursson, P.; Karlsson, J. Correlation between oral drug absorption in humans and apparent drug permeability coefficients in human intestinal epithelial (Caco-2) cells. *Biochem. Biophys. Res. Commun.* **1991**, *175* (3), 880–5.
- (5) Zhu, C.; Jiang, L.; Chen, T. M.; Hwang, K. K. A comparative study of artificial membrane permeability assay for high throughput profiling of drug absorption potential. *Eur. J. Med. Chem.* **2002**, *37* (5), 399–407.
- (6) Seelig, A. The role of size and charge for blood-brain barrier permeation of drugs and fatty acids. *J. Mol. Neurosci.* **2007**, *33* (1), 32–41.
- (7) Avdeef, A. The rise of PAMPA. *Expert Opin. Drug Metab. Toxicol.* **2005**, *1* (2), 325–342.
- (8) Thompson, M.; Lennox, R. B.; McClelland, R. A. Structure and electrochemical properties of microfiltration filter-lipid membrane systems. *Anal. Chem.* **1982**, *54* (1), 76–81.
- (9) Phung, T.; Zhang, Y.; Dunlop, J.; Dalziel, J. E. Porous materials to support bilayer lipid membranes for ion channel biosensors. *Int. J. Electrochem.* **2011**, *2011*, 1–6.
- (10) Wohnsland, F.; Faller, B. High-Throughput Permeability pH Profile and High-Throughput Alkane/Water log P with Artificial Membranes. *J. Med. Chem.* **2001**, *44* (6), 923–930.
- (11) Sugano, K.; Hamada, H.; Machida, M.; Ushio, H. High throughput prediction of oral absorption: Improvement of the composition of the lipid solution used in parallel artificial membrane permeation assay. *J. Biomol. Screening* **2001**, *6* (3), 189–196.
- (12) Avdeef, A.; Tsinman, O. PAMPA - A drug absorption in vitro model. 13. Chemical selectivity due to membrane hydrogen bonding: in combo comparisons of HDM-, DOPC-, and DS-PAMPA models. *Eur. J. Pharm. Sci.* **2006**, *28* (1–2), 43–50.
- (13) Sugano, K.; Takata, N.; Machida, M.; Saitoh, K.; Terada, K. Prediction of passive intestinal absorption using bio-mimetic artificial membrane permeation assay and the paracellular pathway model. *Int. J. Pharm.* **2002**, *241* (2), 241–251.
- (14) Kansy, M.; Senner, F.; Gubernator, K. Physicochemical high throughput screening: parallel artificial membrane permeation assay in

the description of passive absorption processes. *J. Med. Chem.* **1998**, *41* (7), 1007–10.

(15) Seo, P. R.; Teksin, Z. S.; Kao, J. P. Y.; Polli, J. E. Lipid composition effect on permeability across PAMPA. *Eur. J. Pharm. Sci.* **2006**, *29* (3–4), 259–268.

(16) Kansy, M.; Avdeef, A.; Fischer, H. Advances in screening for membrane permeability: high-resolution PAMPA for medicinal chemists. *Drug Discovery Today: Technol.* **2004**, *1* (4), 349–355.

(17) Seelig, J. Lipid polymorphism, reverse micelles, and phosphorus-31 nuclear magnetic resonance. *Reverse Micelles*, [Proc. Eur. Sci. Found. Workshop], 4th **1984**, 209–20.

(18) Morris, K. F.; Johnson, C. S., Jr. Resolution of discrete and continuous molecular size distributions by means of diffusion-ordered 2D NMR spectroscopy. *J. Am. Chem. Soc.* **1993**, *115* (10), 4291–9.

(19) Fischer, H.; Kansy, M.; Avdeef, A.; Senner, F. Permeation of permanently positive charged molecules through artificial membranes—influence of physico-chemical properties. *Eur. J. Pharm. Sci.* **2007**, *31* (1), 32–42.

(20) Stejskal, E. O.; Tanner, J. E. Spin diffusion measurements: spin echoes in the presence of a time-dependent field gradient. *J. Chem. Phys.* **1965**, *42* (1), 288–92.

(21) Wu, D.; Chen, A.; Johnson, C. S., Jr. An improved diffusion-ordered spectroscopy experiment incorporating bipolar-gradient pulses. *J. Magn. Reson., Ser. A* **1995**, *115* (2), 260–4.

(22) Holz, M.; Heil, S. R.; Sacco, A. Temperature-dependent self-diffusion coefficients of water and six selected molecular liquids for calibration in accurate 1H NMR PFG measurements. *Phys. Chem. Chem. Phys.* **2000**, *2* (20), 4740–4742.

(23) Caudwell, D. R.; Trusler, J. P. M.; Vesovic, V.; Wakeham, W. A. The viscosity and density of n-dodecane and n-octadecane at pressures up to 200 MPa and temperatures up to 473 K. *Int. J. Thermophys.* **2004**, *25* (5), 1339–1352.

(24) Avdeef, A.; Stafford, M.; Block, E.; Balogh, M. P.; Chambliss, W.; Khan, I. Drug absorption in vitro model: filter-immobilized artificial membranes. 2. Studies of the permeability properties of lactones in Piper methysticum Forst. *Eur. J. Pharm. Sci.* **2001**, *14* (4), 271–80.

(25) Nielsen, P. E.; Avdeef, A. PAMPA—a drug absorption in vitro model 8. Apparent filter porosity and the unstirred water layer. *Eur. J. Pharm. Sci.* **2004**, *22* (1), 33–41.

(26) Wagner, B.; Fischer, H.; Kansy, M.; Seelig, A.; Assmus, F. Carrier Mediated Distribution System (CAMDIS): a new approach for the measurement of octanol/water distribution coefficients. *Eur. J. Pharm. Sci.* **2015**, *68*, 68–77.

(27) Assmus, F. Artificial Tissue Binding Models: Development and Comparative Evaluation of High-Throughput Lipophilicity Assays and Their Use for PET Tracer Optimization. Thesis; University of Basel: 2015.

(28) Wendel, A. Lecithin. *Kirk-Othmer Encycl. Chem. Technol.* **2000**, DOI: 10.1002/0471238961.1205030923051404.a01.

(29) Yeagle, P. L., Membranes: Phosphorus-31 NMR. In *eMagRes*; John Wiley & Sons, Ltd.: 2007.

(30) Montal, M. Formation of bimolecular membranes from lipid monolayers. *Methods Enzymol.* **1974**, *32*, 545–54.

(31) Gerebtzoff, G.; Seelig, A. In silico prediction of blood-brain barrier permeation using the calculated molecular cross-sectional area as main parameter. *J. Chem. Inf. Model.* **2006**, *46* (6), 2638–50.

(32) Sjoelund, M.; Rilfors, L.; Lindblom, G. Reversed hexagonal phase formation in lecithin-alkane-water systems with different acyl chain unsaturation and alkane length. *Biochemistry* **1989**, *28* (3), 1323–9.

(33) Sjoelund, M.; Lindblom, G.; Rilfors, L.; Arvidson, G. Hydrophobic molecules in lecithin-water systems. I. Formation of reversed hexagonal phases at high and low water contents. *Biophys. J.* **1987**, *52* (2), 145–53.

(34) Kirk, G. L.; Gruner, S. M. Lyotropic effects of alkanes and headgroup composition on the L α -HII lipid liquid crystal phase transition: hydrocarbon packing versus intrinsic curvature. *J. Phys. (Paris)* **1985**, *46* (5), 761–9.

(35) Seelig, A.; Alt, T.; Lotz, S.; Hoelzemann, G. Binding of Substance P Agonists to Lipid Membranes and to the Neurokinin-1 Receptor. *Biochemistry* **1996**, *35* (14), 4365–74.

(36) Montal, M.; Mueller, P. Formation of bimolecular membranes from lipid monolayers and a study of their electrical properties. *Proc. Natl. Acad. Sci. U. S. A.* **1972**, *69* (12), 3561–6.

(37) Luisi, P. L.; Straub, B. E., Eds. *Reverse Micelles: Biological and Technological Relevance of Amphiphilic Structures in Apolar Media*; Plenum Press: 1984.

(38) Schurtenberger, P. Structure and dynamics of viscoelastic surfactant solutions - an application of concepts from polymer science. *Chimia* **1994**, *48* (3), 72–8.

(39) Angelico, R.; Balinov, B.; Ceglie, A.; Olsson, U.; Palazzo, G.; Soderman, O. Water Diffusion in Polymer-like Reverse Micelles. 2. Composition Dependence. *Langmuir* **1999**, *15* (5), 1679–1684.

(40) Ambrosone, L.; Angelico, R.; Ceglie, A.; Olsson, U.; Palazzo, G. Molecular diffusion in a living network. *Langmuir* **2001**, *17* (22), 6822–6830.

(41) Angelico, R.; Palazzo, G.; Olsson, U.; Ambrosone, L.; Ceglie, A. Structural investigation of lecithin/cyclohexane solutions. *Prog. Colloid Polym. Sci.* **1999**, *112* (Trends in Colloid and Interface Science XIII), 1–4.

(42) Scartazzini, R.; Luisi, P. L. Organogels from lecithins. *J. Phys. Chem.* **1988**, *92*, 829–833.

(43) Boguslavsky, V.; Rebecchi, M.; Morris, A. J.; Jhon, D. Y.; Rhee, S. G.; McLaughlin, S. Effect of Monolayer Surface Pressure on the Activities of Phosphoinositide-Specific Phospholipase C- β 1, - γ 1, and - δ 1. *Biochemistry* **1994**, *33* (10), 3032–7.

(44) Xiang, T.-X.; Anderson, B. D. Influence of chain ordering on the selectivity of dipalmitoylphosphatidylcholine bilayer membranes for permeant size and shape. *Biophys. J.* **1998**, *75* (6), 2658–2671.

(45) Nielsen, P. E.; Avdeef, A. PAMPA-a drug absorption in vitro model 8. Apparent filter porosity and the unstirred water layer. *Eur. J. Pharm. Sci.* **2004**, *22* (1), 33–41.

(46) Velicky, M.; Tam, K. Y.; Dryfe, R. A. Permeation of a fully ionized species across a polarized supported liquid membrane. *Anal. Chem.* **2012**, *84* (5), 2541–7.

(47) Seo, P. R.; Teksin, Z. S.; Kao, J. P.; Polli, J. E. Lipid composition effect on permeability across PAMPA. *Eur. J. Pharm. Sci.* **2006**, *29* (3–4), 259–68.

(48) Teksin, Z. S.; Hom, K.; Balakrishnan, A.; Polli, J. E. Ion pair-mediated transport of metoprolol across a three lipid-component PAMPA system. *J. Controlled Release* **2006**, *116* (1), 50–7.

(49) Sugano, K.; Nabuchi, Y.; Machida, M.; Asoh, Y. Permeation characteristics of a hydrophilic basic compound across a bio-mimetic artificial membrane. *Int. J. Pharm.* **2004**, *275* (1–2), 271–8.